Monthly Notices of the ROYAL ASTRONOMICAL SOCIETY

MNRAS **449,** 1380–1390 (2015) doi:10.1093/mnras/stv110

Chromospheric activity and rotational modulation of the RS Canum Venaticorum binary V711 Tauri during 1998–2004

Dongtao Cao[1,2,3★] and Shenghong Gu[1,2]

[1] *Yunnan Observatories, Chinese Academy of Sciences, Kunming 650011, China*
[2] *Key Laboratory for the Structure and Evolution of Celestial Objects, Chinese Academy of Sciences, Kunming 650011, China*
[3] *University of Chinese Academy of Sciences, Beijing 100049, China*

Accepted 2015 January 16. Received 2015 January 16; in original form 2014 August 4

ABSTRACT

We present long-term high-resolution spectroscopic observations of the very active RS Canum Venaticorum-type star V711 Tau, obtained during several observing runs from 1998 to 2004, and study its chromospheric activity. Using the spectral subtraction technique, several optical chromospheric activity indicators [including the He I D_3, Na I D_1, D_2, Hα and Ca II infrared triplet (IRT) lines] formed at different atmospheric heights are analysed. Strong chromospheric emission supports earlier results that indicate that V711 Tau is a very active system. Two large optical flares were detected during our observations. The results suggest that the main part of chromospheric emission is attributed to the primary star of the system. The secondary also presents weak emission but is less active. The ratios of EW_{8542}/EW_{8498} indicate that Ca II IRT emission arises predominantly from plage-like regions. We have found rotational modulation of chromospheric activity in the Hα and Ca II IRT lines, which suggests the presence of the chromospheric active longitudes over the surface of V711 Tau. Two active longitudes separated by about 180° were observed to dominate the activity, and the so-called flip-flop phenomenon was seen during our observations. Moreover, the chromospheric activity level shows a long-term variation that gradually increases from a deep minimum near the year 2002. A close spatial connection of photospheric spots and chromospheric active regions in both short and long timescales was found for V711 Tau.

Key words: stars: activity – binaries: spectroscopic – stars: chromospheres – stars: individual: V711 Tau – stars: late-type.

1 INTRODUCTION

Magnetic activity phenomena, often seen in the Sun, have been widely observed in cool stars. These are very intense due to the deep convection coupled with high rotation rates, resulting in an efficient magnetic dynamo. Rotational rate decreases with age because of the increasing moment of inertia and the loss of angular momentum through magnetic braking during stellar evolution. Thus, the magnetic activity of cool stars indirectly depends on stellar age (Schrijver & Zwaan 2000). At Yunnan Observatories, we began a long-term high-resolution spectroscopic monitoring project for some late-type stars at different evolutionary stages from pre-main sequence stars to evolved stars, to study their magnetic activity (detecting optical flares, searching for prominence-like events, exploring the rotational modulation of chromospheric activity and investigating the evolution of active regions) using the information derived through several optical chromospheric activity indicators formed at different atmospheric heights. In our previous work, we had derived results for one active young main sequence star, LQ Hya, showing that the chromospheric emission exhibits rotational modulation and that the photospheric spots and chromospheric activity regions are spatially connected (Cao & Gu 2014). In the present work, we focus on one of the most active RS Canum Venaticorum binaries, which has at least one evolved component showing remarkable photometric variability caused by photospheric dark spots, chromospheric activity, transition region emission and coronal radiation, V711 Tau.

V711 Tau (HR 1099, HD 22468) is a close double-lined, non-eclipsing spectroscopic binary consisting of a K1 IV primary and a G5 V secondary in an almost circular orbit with a period of about 2.84 d (Fekel 1983). Having a fast rotation rate induced by tidal synchronization and an extended outer convection zone that generates a powerful dynamo, the K1 IV component shows a very high level of magnetic activity. Due to the brightness of the system ($V = 5.7$, Ducati 2002) and extreme magnetic activity, V711 Tau has attracted much attention for nearly all wavelength regions during recent years.

The system always shows significant photometric variability and its long-term star-spot activity has varied cyclically over several years (Henry et al. 1995; Lanza et al. 2006; Berdyugina & Henry

★ E-mail: dtcao@ynao.ac.cn

© 2015 The Authors
Published by Oxford University Press on behalf of the Royal Astronomical Society

Downloaded from http://mnras.oxfordjournals.org/ at National Astronomical Observatory on November 29, 2015

2007; Muneer et al. 2010). Since Vogt & Penrod (1983) published the first Doppler image of V711 Tau, many investigators, e.g. Vogt et al. (1999), Donati (1999), Strassmeier & Bartus (2000), García-Alvarez et al. (2003b), Donati et al. (2003), Petit et al. (2004) and Gu et al. (2007), have studied this very active star using Doppler imaging and found a prominent polar spot concentration over the surface. Furthermore, Berdyugina & Henry (2007) produced the first stellar butterfly diagram of spot activity for V711 Tau and found that the mean latitudes of active regions at opposite longitudes shift antisymmetrically.

The K1 IV star exhibits very intense chromospheric activity, as demonstrated by the Hα emission above the continuum, Ca II H and K, and Ca II infrared triplet (IRT) lines core emission in the optical spectral range (Gondoin 1986; Montes et al. 1995b; Zhai & Zhang 1996; Montes et al. 1997; García-Alvarez et al. 2003a). V711 Tau has frequently been observed by the MUSICOS (Multi-Site Continuous Spectroscopy) project, which has acquired a continuous spectroscopic coverage over several days. Foing et al. (1994) observed the modulation of the Ca II K line profile due to chromospheric plage-like regions and found two white-light flares during the MUSICOS 1989 campaign. García-Alvarez et al. (2003a) obtained continuous observations of several chromospheric activity indicators during the MUSICOS 1998 campaign and detected two large optical flares. Both flares were in the same active region. Rotational modulation was also found in the Hα and He I D$_3$ lines, which was anti-correlated with the photometric light curves.

Although there have been many papers on the magnetic activity of V711 Tau, long-term chromospheric activity studies and simultaneous analysis of several chromospheric activity indicators are rare. It is very important to understand the vertical structure of active regions and their evolution. In this paper, we present the results of the short-term (rotational modulation) and long-term chromospheric activity of V711 Tau, based on a large set of high-resolution spectroscopic observations from 1998 to 2004. Moreover, we compare our results with nearly simultaneous light curves observed by other authors to investigate the possible correlation between photometric and chromospheric activity regions.

The details of our observations and data reduction are given in Section 2, and the procedure for the spectral analysis is described in Section 3. In Section 4, the behaviour of chromospheric activity indicators, the variation of chromospheric activity, and the correlation between photospheric spots and chromospheric activity are discussed. Finally, we state the conclusions of our study in Section 5.

2 OBSERVATIONS AND DATA REDUCTION

Spectroscopic observations of V711 Tau were performed during several observing seasons from 1998 to 2004. The observations were carried out with the 2.16-m telescope at the Xinglong station of the National Astronomical Observatories, China. The Coudé echelle spectrograph with a resolving power of about 37 000 and a 1024 × 1024-pixel Tektronix CCD detector were used (Zhao & Li 2001). The reciprocal dispersions are 0.082 Å pixel^{-1} for the Na I D$_1$, D$_2$, He I D$_3$ spectral region, 0.091 Å pixel^{-1} for the Hα spectral region, 0.118 Å pixel^{-1} for the Ca II $\lambda\lambda$8498, 8542 spectral region, and 0.120 Å pixel^{-1} for the Ca II λ8662 spectral region. Correspondingly, the spectral resolution determined as the full width at half-maximum of the arc comparison lines is 0.152, 0.167, 0.211 and 0.216 Å, respectively.

In Table 1, we give the observing log, which includes the observing date, the heliocentric Julian date (HJD), orbital phase

Table 1. Observing log of V711 Tau.

Date	HJD[a] (2 450 000+)	Phase	Exposure time (s)
1998 Mar 13	0885.9641	0.3911	720
1998 Mar 13	0885.9740	0.3946	720
2000 Feb 19	1594.0815	0.9268	1200
2000 Feb 20	1595.0730	0.2762	1200
2000 Feb 21	1596.0773	0.6301	1200
2000 Feb 22	1597.0391	0.9691	1200
2000 Feb 23	1598.0356	0.3202	1200
2000 Feb 24	1599.0312	0.6711	1200
2000 Sept 15	1803.2550	0.6381	1200
2000 Sept 16	1804.2564	0.9910	1200
2000 Sept 17	1805.2357	0.3361	1200
2001 Nov 23	2237.1026	0.5230	1200
2001 Nov 24	2238.1337	0.8864	2700
2001 Nov 25	2239.0943	0.2249	1800
2001 Nov 25	2239.3069	0.2998	1500
2001 Nov 26	2240.0637	0.5665	1800
2001 Nov 27	2241.0928	0.9292	900
2001 Nov 29	2243.1581	0.6570	1800
2001 Dec 01	2245.1479	0.3581	1800
2002 Dec 13	2622.0042	0.1597	1200
2002 Dec 13	2622.1209	0.2008	1200
2002 Dec 13	2622.2390	0.2424	1200
2002 Dec 16	2624.9965	0.2142	1500
2002 Dec 16	2625.1684	0.2747	1800
2002 Dec 17	2626.0329	0.5794	1800
2002 Dec 17	2626.1992	0.6380	1800
2003 Nov 08	2952.1053	0.4851	900
2003 Nov 08	2952.1162	0.4889	900
2003 Nov 08	2952.2523	0.5368	900
2003 Nov 08	2952.2629	0.5406	900
2003 Nov 08	2952.3489	0.5709	1800
2003 Nov 10	2954.2100	0.2267	900
2003 Nov 10	2954.2208	0.2305	900
2003 Nov 10	2954.3351	0.2708	900
2003 Nov 10	2954.3459	0.2746	900
2004 Feb 03	3039.1104	0.1450	600
2004 Feb 04	3040.0640	0.4811	900
2004 Feb 04	3040.0749	0.4849	900
2004 Feb 05	3041.0323	0.8223	600
2004 Feb 05	3041.0395	0.8248	600
2004 Feb 06	3042.1073	0.2011	900
2004 Feb 06	3042.1182	0.2050	900
2004 Feb 07	3043.0752	0.5422	600
2004 Feb 07	3043.0825	0.5448	600
2004 Feb 08	3044.0365	0.8810	600
2004 Feb 08	3044.0444	0.8838	600
2004 Feb 09	3045.0515	0.2386	600
2004 Feb 09	3045.0588	0.2412	600
2004 Nov 20	3330.2409	0.7374	600
2004 Nov 20	3330.2481	0.7400	600
2004 Nov 21	3331.2181	0.0818	900
2004 Nov 21	3331.2290	0.0856	900
2004 Nov 22	3332.3337	0.4749	1200
2004 Nov 25	3335.2975	0.5193	3600
2004 Nov 26	3336.2707	0.8623	1200
2004 Nov 26	3336.2852	0.8674	1200
2004 Nov 26	3336.2994	0.8724	1200
2004 Nov 26	3336.3136	0.8774	1200
2004 Nov 27	3337.2215	0.1974	600
2004 Nov 27	3337.2292	0.2000	600

Downloaded from http://mnras.oxfordjournals.org/ at National Astronomical Observatory on November 29, 2015

Table 1. – *continued*

Date	HJD[a] (2 450 000+)	Phase	Exposure time (s)
2004 Nov 27	3337.2364	0.2026	600
2004 Nov 27	3337.2865	0.2202	600
2004 Nov 27	3337.2959	0.2236	900
2004 Nov 27	3337.3068	0.2274	900
2004 Nov 28	3338.0829	0.5009	2700
2004 Nov 29	3339.2097	0.8980	1800
2004 Nov 29	3339.2970	0.9287	3000

Note. [a]Heliocentric Julian date.

and exposure time. The orbital phases were calculated with the ephemeris:

$$\mathrm{HJD_{conj}} = 2442\,766.080 + 2\overset{\mathrm{d}}{.}837\,74 \times E, \tag{1}$$

from Fekel (1983), where zero phase corresponds to the conjunction with the K1 IV primary in front. In total, 67 spectra of V711 Tau were obtained. In addition, observations of some early-type stars and non-active stars were obtained. The spectra of early-type stars were used as telluric templates whereas the non-active stars were used as reference stars in the spectral subtraction technique.

The spectrum reduction was performed with the IRAF package,[1] following the standard reduction procedures (image trimming, bias correction, flat-field division, scattered light subtraction, one-dimensional spectrum extraction and wavelength calibration). The wavelength was calibrated using the spectra of a Th-Ar lamp. Finally, all spectra were normalized using a low-order polynomial fit to the observed continuum. The signal-to-noise ratio (S/N) is more than 100 in the chromospheric activity indicator regions for most of our observations. In Fig. 1, we display the normalized Ca II IRT (λ8662, λ8542 and λ8498), Hα, He I D_3, and Na I D_1, D_2 line profiles of V711 Tau obtained during our observations. The orbital phase and observing date are also marked in the figure. During the 1998 observing run, the Ca II IRT λ8498 line was not in the spectra due to the echelle frame position change.

For some observations during which telluric water vapour lines were heavy in the chromospheric activity line regions, two rapidly rotating early-type stars HR 7894 (B5 IV, $v\sin i = 330$ km s^{-1}) and HR 8858 (B 5V, $v\sin i = 332$ km s^{-1}) were used as telluric templates. The telluric lines in the spectra of V711 Tau are eliminated using these templates with an interactive procedure, as described by Gu et al. (2002) in detail.

3 SPECTRAL ANALYSIS

To obtain the pure chromospheric contribution, we apply a method usually called the spectral subtraction technique, which was described in detail by Barden (1985) and Montes et al. (1995a). This method has been widely and successfully used for chromospheric activity studies (Gunn & Doyle 1997; Gunn, Doyle & Houdebine 1997; Montes et al. 1995b, 1997, 2000; Gu et al. 2002; Zhang & Gu 2008; Cao & Gu 2012, 2014). It subtracts a synthesized spectrum constructed from artificially rotationally broadened, radial velocity shifted, and weighted spectra of two inactive stars with the same spectral type and luminosity class as the two components of the binary system. The synthesized spectrum represents the contribution of the non-active state of the system, and the subtraction between the observed and the synthesized spectra provides the pure chromospheric activity emission caused by activity. Here, the synthesized spectra were constructed using the program STARMOD (Barden 1985).

During our observations, we observed some stars with spectral types and luminosity classes similar to the components of V711 Tau as candidate reference stars. By comparison, HR 7690 (K1 IV) and HR 7683 (G5 IV) were used in the synthesized spectrum construction. The $v\sin i$ value of each component of V711 Tau was determined using the reference spectrum in the course of the spectral analysis. According to the method described in detail by Barden (1985), average values of 41.5 km s^{-1} for the primary and 8.5 km s^{-1} for the secondary were obtained from high S/N spectra, spanning the wavelength regions 6030–6220 Å, 6370–6520 Å and 6590–6670 Å with many photospheric lines, at phases where the two components were well separated. The obtained value for the primary is in good agreement with the one estimated by Donati et al. (1992), Vogt et al. (1999), Donati (1999) and Strassmeier & Bartus (2000). Moreover, the adopted intensity weight ratios are 0.745/0.255 for the Na I D_1, D_2, He I D_3 spectral region, 0.76/0.24 for the Hα spectral region, 0.77/0.23 for the Ca II λλ8498, 8542 spectral region, and 0.78/0.22 for the Ca II λ8662 spectral region. Consequently, the synthesized spectra were constructed by broadening and weighting the reference spectra to the values of $v\sin i$ and the intensity weight ratios derived above, and shifting along the radial-velocity axis. Finally, the subtracted spectra were calculated for V711 Tau. Examples of spectral subtraction in the Ca II IRT (λ8662, λ8542 and λ8498), Hα, Na I D_1, D_2, and He I D_3 line spectral regions at phase 0.2202 on 2004 November 27 are presented in Fig. 2.

For the primary component, the equivalent widths (EWs) of the excess emission in the different chromospheric diagnostics were measured for the subtracted spectra using the IRAF/SPLOT task. We determined the EWs by integrating over the emission profiles in the subtracted spectra, and additionally measured them using a Gaussian function fit. To measure the EWs of asymmetric profiles more accurately, we may need more Gaussian profiles to fit them. The final EWs for the Ca II IRT (λ8662, λ8542 and λ8498) and Hα lines were derived by taking the mean values of the two methods and are listed in Table 2 along with their errors. The errors for the measured EWs were estimated by using the difference between the measurements of the two methods. In Table 2 we also give the ratio of excess emission, EW_{8542}/EW_{8498}, which is used as an indicator of the type of chromospheric structure that produces the observed Ca II IRT emission.

Finally, to analyse the possible rotational modulation of chromospheric activity of V711 Tau, the observations of each observing run were grouped together. We plot the EWs of Hα and Ca II IRT excess emission as a function of orbital phase in Fig. 3.

4 DISCUSSION

4.1 Chromospheric activity indicators

Chromospheric activity lines formed at different atmospheric heights were obtained for V711 Tau during our observations, such as the Hα (formed in the middle chromosphere), Na I D_1, D_2 (upper photosphere and lower chromosphere), He I D_3 (upper chromosphere), and Ca II IRT (lower chromosphere) lines. These lines have been proven to be very important and useful chromospheric activity

[1] IRAF is distributed by the National Optical Astronomy Observatories, which is operated by the Association of Universities for Research in Astronomy (AURA), Inc, under cooperative agreement with the National Science Foundation.

Downloaded from http://mnras.oxfordjournals.org/ at National Astronomical Observatory on November 29, 2015

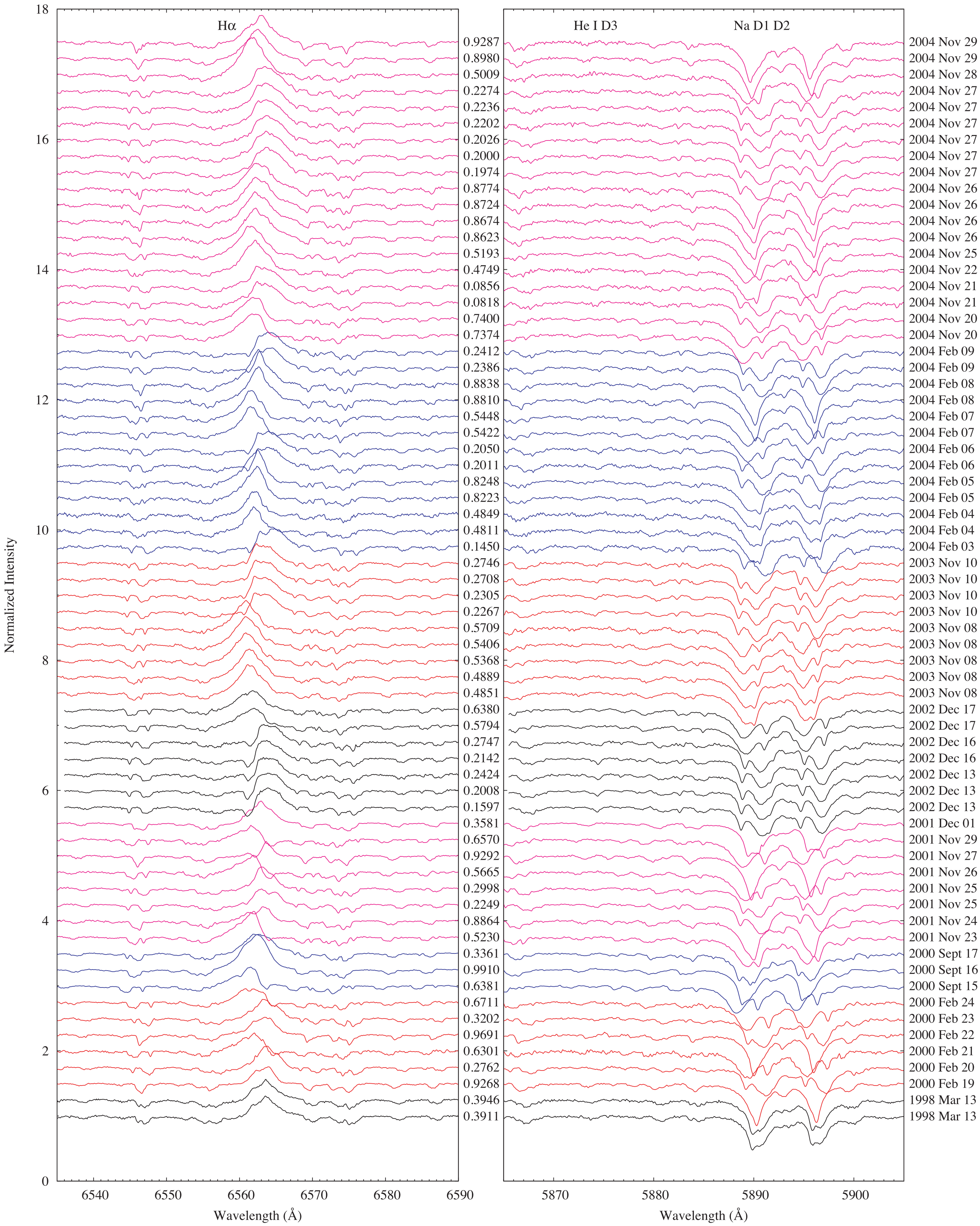

Figure 1. Hα, Na I D_1, D_2, He I D_3 and Ca II IRT (λ8662, λ8542 and λ8498) line profiles of V711 Tau obtained during our observations from 1998 to 2004, and shifted arbitrarily. The different observing runs are plotted with different colours for better visibility.

Downloaded from http://mnras.oxfordjournals.org/ at National Astronomical Observatory on November 29, 2015

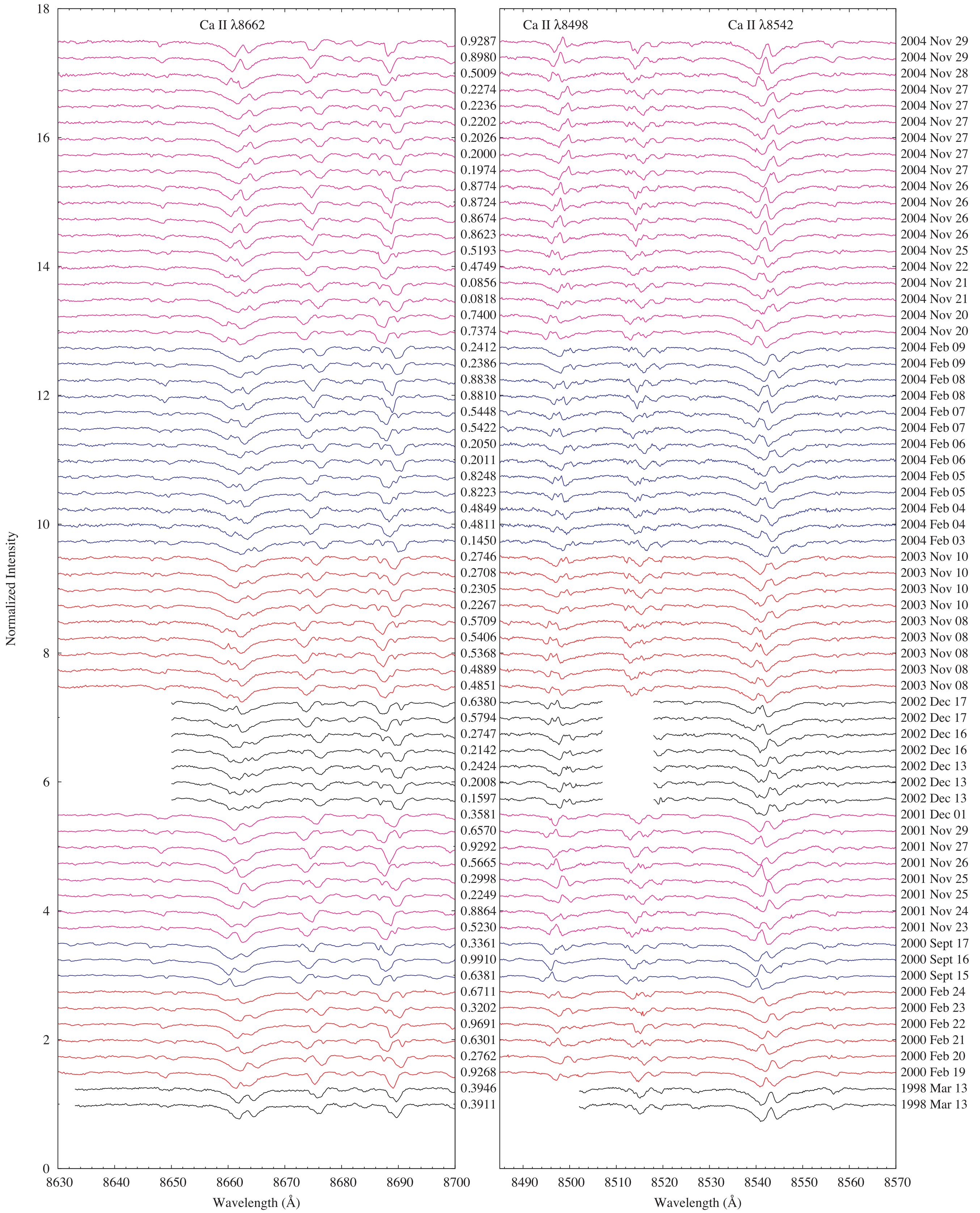

Figure 1. – *continued*

Downloaded from http://mnras.oxfordjournals.org/ at National Astronomical Observatory on November 29, 2015

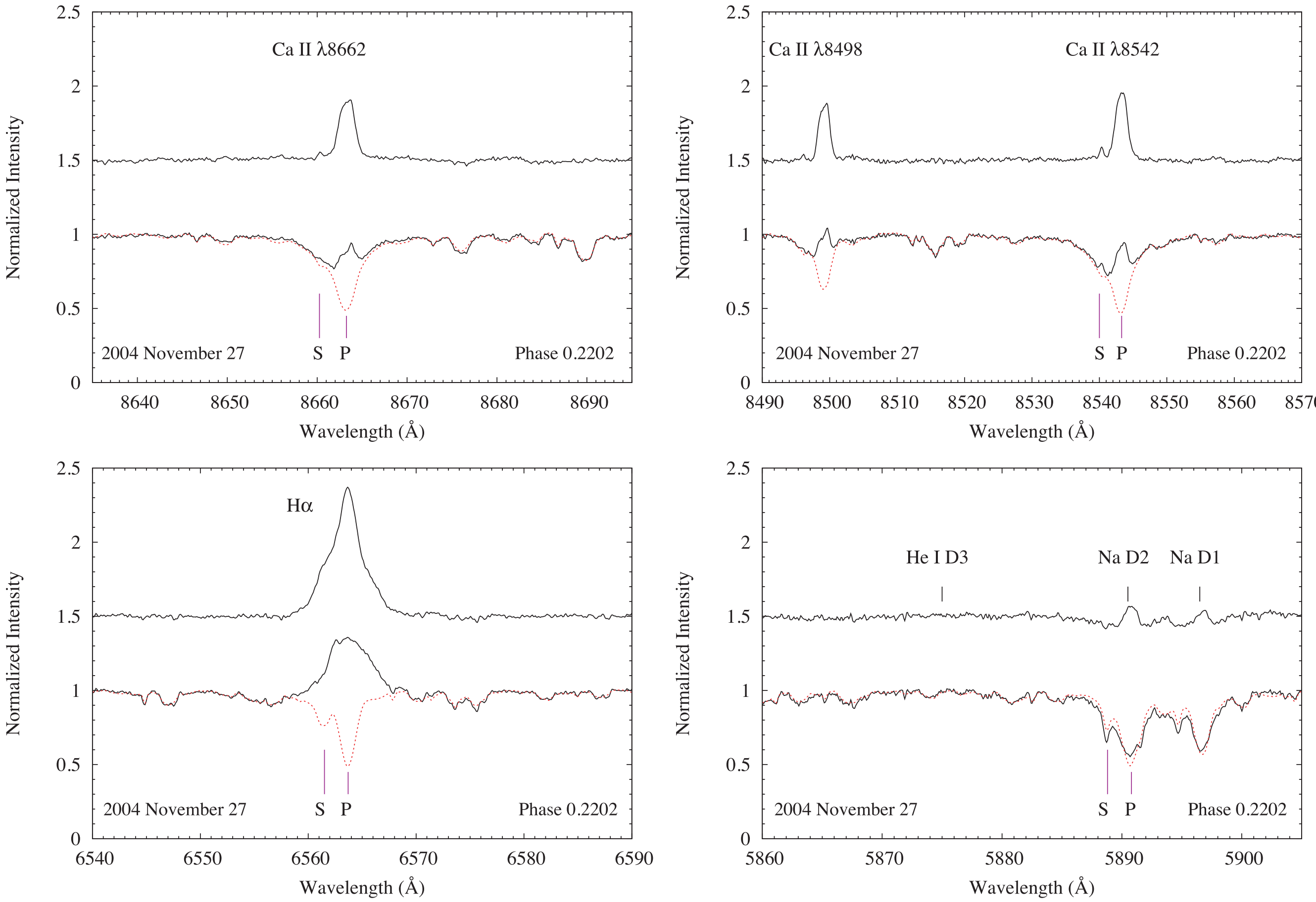

Figure 2. Examples of the observed, synthesized and subtracted spectra for the Ca II IRT (λ8662, λ8542 and λ8498), Hα, Na I D_1, D_2, and He I D_3 line spectral regions. For each panel, the lower solid line is the observed spectrum, the dotted line represents the synthesized spectrum and the upper spectrum is the subtracted one, shifted for better display. 'P' and 'S' indicate the primary and secondary components of the system, respectively.

indicators in the optical spectral range from the region of low temperature to the upper chromosphere (Gunn & Doyle 1997; Gunn et al. 1997; Montes et al. 1995b, 1997, 2000), which can help us to investigate the chromospheric structure for different atmospheric layers.

In Fig. 1, V711 Tau always shows Hα in emission above the continuum, and has a very variable profile. In all spectra, we can see clear emission reversals in the cores of the Ca II IRT absorption line profiles. Moreover, asymmetry of the chromospheric emission profiles and the profiles with central absorption reversal appeared in the Ca II IRT lines at most phases. Gondoin (1986) found a similar structure in the Ca II IRT lines of V711 Tau and concluded that the polar chromospheric plages located on the primary star could account for this feature. At phases such as 0.2202 on 2004 November 27 where the two components were well separated, it can be seen that weak emission features appear near the main core emission in Ca II IRT lines, especially in the Ca II λ8542 line.

The synthesized spectra match the observational ones quite well (see Fig. 2). The exceptions are the Na I D_1, D_2 lines, which are very sensitive to the effective temperature. Just a slight temperature difference between the target and reference stars can produce significant changes in the wings of the line profiles. Despite that, according to Montes et al. (1997), the filled-in cores of the Na I D_1, D_2 lines could be used as chromospheric activity indicators. After application of the spectral subtraction technique, one can see that the Ca II IRT, Hα and Na I D_1, D_2 excess emission is primarily associated with the K1 IV star. Moreover, it is clearly seen that the weak emission features in the Ca II IRT line profiles arose from the G5 V secondary star (see Fig. 2). This is consistent with the emission in the Ca II H and K lines found by Montes et al. (1995b), which suggests that the secondary is also active, but less active than the primary star.

The Hα line profile shows broad emission wings, consistent with the findings by Montes et al. (1997), which can arise from microflaring in the chromosphere. Moreover, broad wings in the chromospheric Mg II *h* and *k* lines of V711 Tau were also detected by Dempsey et al. (1996) and Wood et al. (1996). Such broad emission wings had been found previously for several other chromospheric active stars (Montes et al. 2000; Gu et al. 2002; Zhang & Gu 2008).

For the ratio of excess emission EW_{8542}/EW_{8498}, we find the values in the range 1–2 (see Table 2), approximating the values in solar plages (∼1.5–3; Chester 1991), which indicate that Ca II IRT emission arises predominantly from plage-like regions. These low values have also been found for several other chromospheric active stars by many authors, e.g. Montes et al. (2000), Gu et al. (2002), López-santiago et al. (2003), Zhang & Gu (2008), Gálvez et al. (2009) and Cao & Gu (2014).

4.2 Optical flares

The He I D_3 line emission is the most important evidence in support of the occurrence of an optical flare (Zirin 1988). As shown in

Downloaded from http://mnras.oxfordjournals.org/ at National Astronomical Observatory on November 29, 2015

Table 2. Measurements for excess emission of the Ca II IRT and Hα lines in the subtracted spectra.

Date	Phase	$EW_{\lambda 8498}$ (Å)	$EW_{\lambda 8542}$ (Å)	$EW_{\lambda 8662}$ (Å)	$EW_{H\alpha}$ (Å)	EW_{8542}/EW_{8498}
1998 Mar	0.3911	...	1.074 ± 0.011	0.974 ± 0.012	2.629 ± 0.011	...
	0.3946	...	1.072 ± 0.011	0.976 ± 0.011	2.592 ± 0.009	...
2000 Feb	0.9268	0.694 ± 0.002	0.931 ± 0.008	0.832 ± 0.002	2.358 ± 0.012	1.341
	0.2762	0.678 ± 0.002	0.951 ± 0.013	0.853 ± 0.002	2.505 ± 0.005	1.403
	0.6301	0.698 ± 0.003	0.985 ± 0.015	0.862 ± 0.003	2.379 ± 0.004	1.411
	0.9691	0.682 ± 0.001	0.917 ± 0.005	0.821 ± 0.001	2.631 ± 0.013	1.345
	0.3202	0.667 ± 0.005	0.930 ± 0.001	0.814 ± 0.007	2.565 ± 0.008	1.394
	0.6711	0.651 ± 0.007	0.964 ± 0.002	0.842 ± 0.010	2.184 ± 0.006	1.481
2000 Sept	0.6381	0.801 ± 0.015	1.237 ± 0.025	1.093 ± 0.012	2.474 ± 0.006	1.544
	0.9910	0.749 ± 0.015	1.108 ± 0.023	0.881 ± 0.020	3.989 ± 0.011	1.479
	0.3361	0.647 ± 0.011	0.939 ± 0.012	0.768 ± 0.023	2.951 ± 0.009	1.451
2001 Nov–Dec	0.5230	0.786 ± 0.011	1.111 ± 0.025	1.053 ± 0.039	2.700 ± 0.020	1.413
	0.8864	0.664 ± 0.012	0.885 ± 0.011	0.829 ± 0.016	2.213 ± 0.005	1.333
	0.2249	0.724 ± 0.023	1.044 ± 0.023	0.884 ± 0.024	2.331 ± 0.018	1.442
	0.2998	0.806 ± 0.018	1.059 ± 0.025	0.955 ± 0.015	2.423 ± 0.035	1.314
	0.5665	0.819 ± 0.022	1.083 ± 0.023	0.978 ± 0.010	2.117 ± 0.020	1.322
	0.9292	0.692 ± 0.021	0.861 ± 0.012	0.821 ± 0.015	1.866 ± 0.030	1.244
	0.6570	0.714 ± 0.020	0.992 ± 0.013	0.893 ± 0.025	1.913 ± 0.020	1.389
	0.3581	0.724 ± 0.013	1.065 ± 0.030	0.946 ± 0.020	2.689 ± 0.025	1.471
2002 Dec	0.1597	0.717 ± 0.004	0.937 ± 0.017	0.838 ± 0.014	2.303 ± 0.019	1.307
	0.2008	0.724 ± 0.004	0.958 ± 0.013	0.848 ± 0.015	2.364 ± 0.015	1.323
	0.2424	0.682 ± 0.025	0.916 ± 0.012	0.836 ± 0.013	2.314 ± 0.015	1.343
	0.2142	0.668 ± 0.002	0.860 ± 0.011	0.809 ± 0.011	2.199 ± 0.011	1.287
	0.2747	0.702 ± 0.005	0.938 ± 0.019	0.815 ± 0.012	2.380 ± 0.005	1.336
	0.5794	0.711 ± 0.001	0.998 ± 0.020	0.904 ± 0.007	2.527 ± 0.020	1.404
	0.6380	0.721 ± 0.001	1.023 ± 0.025	0.927 ± 0.016	2.680 ± 0.033	1.419
2003 Nov	0.4851	0.702 ± 0.011	0.987 ± 0.024	0.849 ± 0.013	3.147 ± 0.003	1.406
	0.4889	0.704 ± 0.012	0.980 ± 0.015	0.834 ± 0.013	3.118 ± 0.025	1.392
	0.5368	0.711 ± 0.010	0.980 ± 0.010	0.844 ± 0.014	3.135 ± 0.011	1.378
	0.5406	0.706 ± 0.011	1.012 ± 0.023	0.839 ± 0.016	3.065 ± 0.012	1.433
	0.5709	0.705 ± 0.014	0.985 ± 0.012	0.841 ± 0.023	2.904 ± 0.011	1.397
	0.2267	0.682 ± 0.013	0.982 ± 0.013	0.877 ± 0.028	2.473 ± 0.010	1.440
	0.2305	0.685 ± 0.010	0.989 ± 0.022	0.899 ± 0.013	2.497 ± 0.015	1.444
	0.2708	0.672 ± 0.011	1.000 ± 0.030	0.867 ± 0.013	2.520 ± 0.015	1.488
	0.2746	0.663 ± 0.011	1.001 ± 0.025	0.894 ± 0.021	2.459 ± 0.008	1.510
2004 Feb	0.1450	0.630 ± 0.019	0.945 ± 0.015	0.889 ± 0.017	2.441 ± 0.012	1.50
	0.4811	0.680 ± 0.012	0.946 ± 0.012	0.861 ± 0.019	2.420 ± 0.025	1.391
	0.4849	0.642 ± 0.011	0.945 ± 0.019	0.862 ± 0.011	2.400 ± 0.013	1.472
	0.8223	0.710 ± 0.014	1.141 ± 0.022	0.932 ± 0.019	3.002 ± 0.018	1.607
	0.8248	0.714 ± 0.014	1.131 ± 0.031	0.945 ± 0.015	3.024 ± 0.019	1.584
	0.2011	0.609 ± 0.015	0.914 ± 0.013	0.865 ± 0.021	2.415 ± 0.015	1.501
	0.2050	0.640 ± 0.011	0.944 ± 0.012	0.876 ± 0.022	2.353 ± 0.013	1.475
	0.5422	0.718 ± 0.012	0.975 ± 0.011	0.871 ± 0.011	2.643 ± 0.024	1.358
	0.5448	0.728 ± 0.012	0.985 ± 0.011	0.883 ± 0.012	2.631 ± 0.011	1.353
	0.8810	0.719 ± 0.013	1.134 ± 0.012	0.968 ± 0.012	3.244 ± 0.014	1.577
	0.8838	0.711 ± 0.012	1.126 ± 0.012	0.967 ± 0.012	3.275 ± 0.015	1.584
	0.2386	0.691 ± 0.014	0.941 ± 0.016	0.880 ± 0.021	2.491 ± 0.012	1.362
	0.2412	0.694 ± 0.012	0.950 ± 0.012	0.866 ± 0.022	2.439 ± 0.019	1.369
2004 Nov	0.7374	0.715 ± 0.031	0.995 ± 0.035	0.963 ± 0.021	2.599 ± 0.012	1.392
	0.7400	0.702 ± 0.021	1.022 ± 0.034	0.928 ± 0.023	2.553 ± 0.013	1.456
	0.0818	0.666 ± 0.012	1.002 ± 0.023	0.906 ± 0.014	2.798 ± 0.016	1.505
	0.0856	0.702 ± 0.016	1.015 ± 0.021	0.933 ± 0.017	2.697 ± 0.015	1.446
	0.4749	0.723 ± 0.021	1.123 ± 0.014	0.978 ± 0.021	3.152 ± 0.013	1.553
	0.5193	0.725 ± 0.013	1.093 ± 0.023	0.956 ± 0.019	3.137 ± 0.014	1.508
	0.8623	0.780 ± 0.022	1.149 ± 0.019	0.999 ± 0.015	3.301 ± 0.013	1.473
	0.8674	0.784 ± 0.015	1.144 ± 0.014	0.973 ± 0.015	3.358 ± 0.028	1.459
	0.8724	0.802 ± 0.014	1.155 ± 0.021	1.013 ± 0.017	3.224 ± 0.019	1.440
	0.8774	0.801 ± 0.023	1.145 ± 0.011	1.007 ± 0.022	3.169 ± 0.019	1.429
	0.1974	0.742 ± 0.019	1.137 ± 0.013	0.964 ± 0.021	3.062 ± 0.022	1.532
	0.2000	0.769 ± 0.014	1.104 ± 0.021	0.949 ± 0.011	3.062 ± 0.022	1.436
	0.2026	0.762 ± 0.023	1.138 ± 0.011	0.971 ± 0.020	3.059 ± 0.017	1.493
	0.2202	0.760 ± 0.017	1.086 ± 0.021	0.969 ± 0.019	3.107 ± 0.018	1.429

Downloaded from http://mnras.oxfordjournals.org/ at National Astronomical Observatory on November 29, 2015

Table 2. – *continued*

Date	Phase	$EW_{\lambda 8498}$ (Å)	$EW_{\lambda 8542}$ (Å)	$EW_{\lambda 8662}$ (Å)	$EW_{H\alpha}$ (Å)	EW_{8542}/EW_{8498}
2004 Nov	0.2236	0.751 ± 0.021	1.102 ± 0.016	0.988 ± 0.025	3.090 ± 0.013	1.467
	0.2274	0.737 ± 0.015	1.100 ± 0.018	0.986 ± 0.016	3.080 ± 0.022	1.493
	0.5009	0.768 ± 0.022	1.156 ± 0.023	1.022 ± 0.023	3.734 ± 0.012	1.505
	0.8980	0.868 ± 0.014	1.180 ± 0.012	1.069 ± 0.017	3.255 ± 0.023	1.359
	0.9287	0.826 ± 0.019	1.103 ± 0.012	1.048 ± 0.023	3.112 ± 0.011	1.335

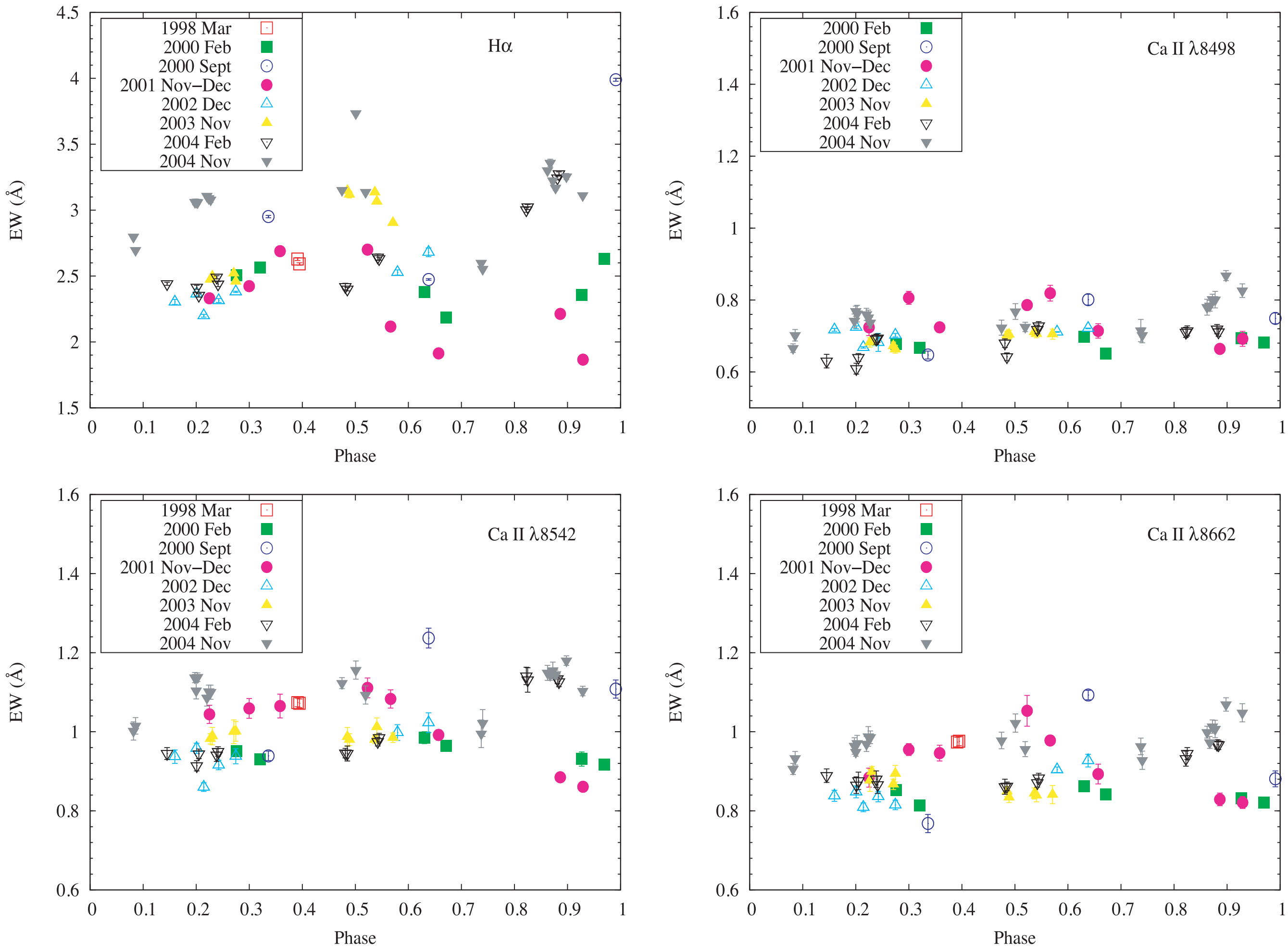

Figure 3. EWs of excess emission versus orbital phase for Hα and Ca II IRT lines. The label identifying each observing run and chromospheric activity indicator are marked in the corresponding plot.

Fig. 4, in which the He I D_3 lines show weak emission, two optical flares occurred on V711 Tau during our observations. The first flare happened on 2000 September 16 (HJD 2451 804.2564) at phase 0.9901. The second one occurred on 2004 November 28 (HJD 2453 338.0829) at phase 0.5009.

When the two flares happened, the Hα line strengthened dramatically (see Figs 1 and 4). The intensity of the Hα emission is stronger than the emission of the first optical flare detected by García-Alvarez et al. (2003a) in 1998 November. Calculating the stellar continuum flux in the Hα line region using the calibration of Hall (1996) and the colour index $B - V = 0.92$ of V711 Tau (Eggen 1978), and converting the EWs into the absolute flux at the stellar surface, we have estimated the flare energy in the observed Hα line as 1.7×10^{31} erg s^{-1} for the first flare and 1.59×10^{31} erg s^{-1} for the second one. We corrected the EWs to the total continuum before they were converted to the absolute flux at the stellar surface. The values for energy released in the Hα line during the flares have a similar order of magnitude to the ones for V711 Tau estimated by García-Alvarez et al. (2003a) and for UX Ari calculated by Gu et al. (2002).

4.3 Rotational modulation and active longitudes

Variability of chromospheric emission with orbital phase indicates that the distribution of active regions is not uniformly seen on the stellar surface. Rotational modulation of chromospheric activity can help us to derive the location of active regions, similar to the hot solar plage structures, and has been found in many active stars using several chromospheric diagnostics (Berdyugina, Ilyin & Tuominen

Downloaded from http://mnras.oxfordjournals.org/ at National Astronomical Observatory on November 29, 2015

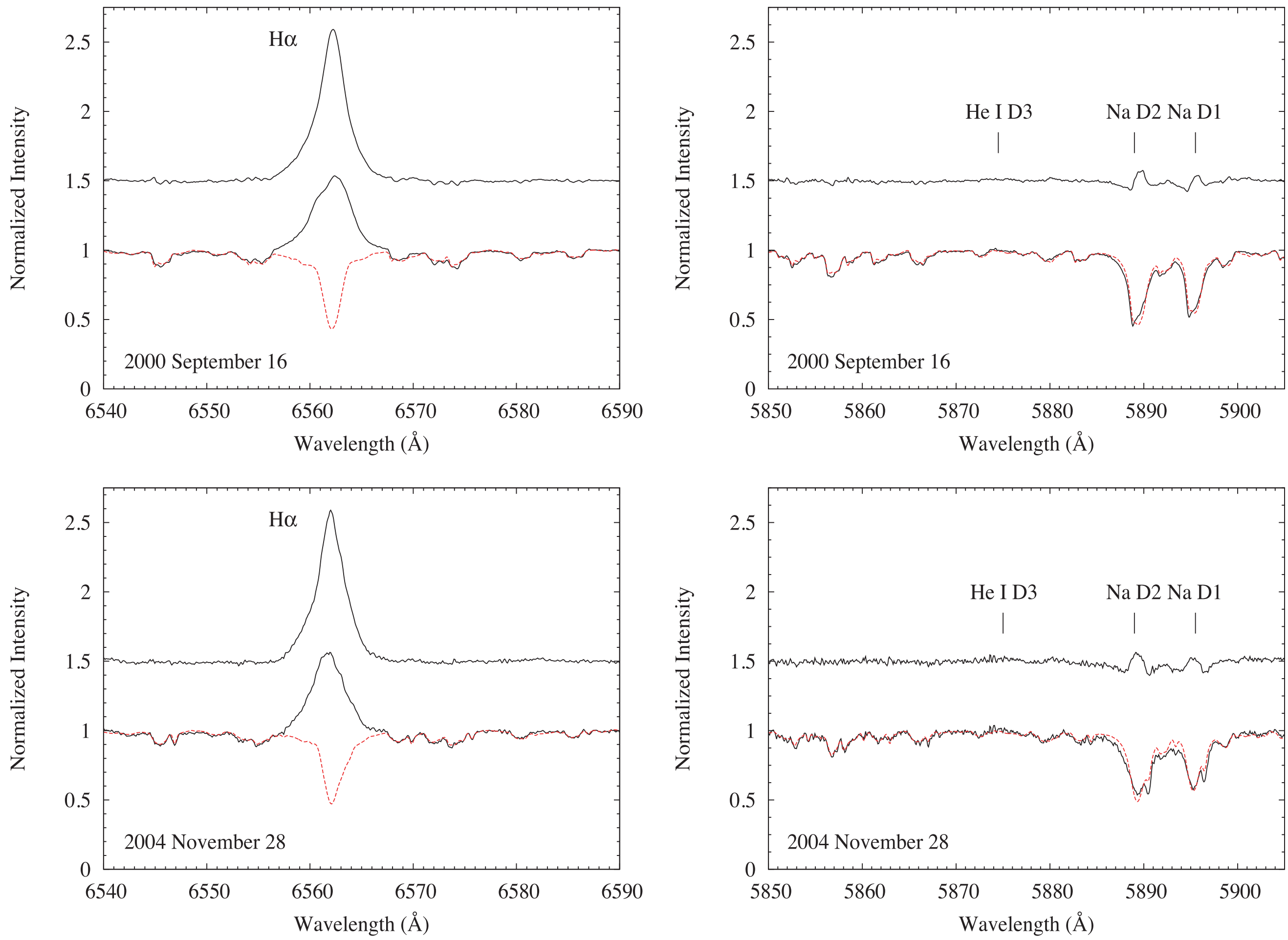

Figure 4. He I D_3, Na I D_1, D_2 and Hα lines during flares.

1999; Gu et al. 2002; García-Alvarez et al. 2003a; Frasca et al. 2008a,b; Zhang & Gu 2008).

The observing runs of 2000 February, 2001 November to December, 2004 February and 2004 November had better orbital phase coverage during our observations. From Fig. 3, it can be seen that the EWs of Hα and Ca II IRT excess emission correlate and show rotational modulation. This suggests the presence of active longitudes over the surface of V711 Tau. In 2000 February, although only six spectra were observed, there is a clearly modulated trend showing two active longitudes: one chromospheric activity longitude occurs at phase between 0.3 and 0.6, while another active longitude exists around phase 1.0. For the 2001 observing run, the activity variation indicates a strong active longitude appears near phase 0.4, and a narrow active longitude near phase 0.9. For 2004 November, we notice that there are two active longitudes located near phases 0.4 and 0.9. However, although there is a gap between 0.25 and 0.5 in 2004 February, the overall level of the chromospheric variation is flat and weak compared with the 2004 November observing run for the first active longitude. The active longitude at the second half of the orbital phase seems to be stronger. This may indicate that the chromospheric activity regions evolved dramatically between those two observing runs in 2004.

We find two surviving chromospheric activity longitude regions, a broader, primary activity longitude and a narrower, secondary longitude separated about 180°, which dominate the activity of V711 Tau during our observations, except the observation in 2004 February. For V711 Tau, Berdyugina & Henry (2007) analysed photometric data for the years 1975–2006 with an inversion technique and found that spot phases constitute two migrating active longitudes separated by 180° on average. A similar feature with two active longitudes has also been found for V711 Tau by Lanza et al. (2006), and in other active RS Canum Venaticorum (CVn)-type binary systems (Berdyugina et al. 1998; Gu et al. 2002; Zhang & Gu 2008) and rapidly rotating single stars, such as LQ Hya (Berdyugina, Pelt & Tuominen 2002). According to the change of the dominating activity longitude between opposite hemispheres in 2004 February and November, moreover, we infer that a flip-flop phenomenon occurred in chromospheric activity regions of V711 Tau, which suggests the redistribution of active regions. The flip-flop cycle with a period of 5.3 ± 0.1 yr for V711 Tau was derived by Berdyugina & Henry (2007) from cyclic pattern of the peak-to-peak V magnitude. A similar short-term spot activity cycle with a period of 3–5 yr was also reported by Lanza et al. (2006). Moreover, Buccino & Mauas (2009) found a chromospheric flip-flop cycle with a period of ~3.3 yr through analysing the peak-to-peak Mount Wilson index for several seasons.

4.4 Correlation between photospheric spots and chromospheric activity

There is close spatial connection between photospheric spots and chromospheric plages for most single active stars and RS CVn-type

Downloaded from http://mnras.oxfordjournals.org/ at National Astronomical Observatory on November 29, 2015

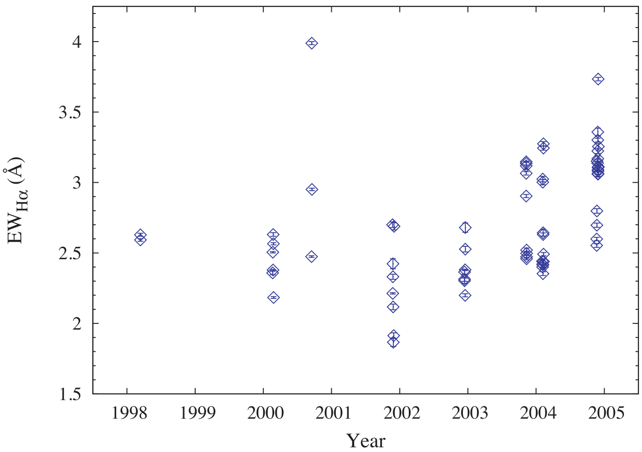

Figure 5. Hα chromospheric activity emission of V711 Tau versus year for all observations.

systems. For example, Catalano et al. (1996) found that the variation of chromospheric activity is anti-correlated with the optical light curve for V711 Tau and several other active binaries, which indicates that the chromospheric activity regions are mainly concentrated in regions above dark spots.

According to Lanza et al. (2006), the timescale for the evolution of the spot pattern is of the order of 100–200 d and their individual light curves were built with this time baseline. Our observing runs in 2000 February and 2001 November–December overlapped with their observations for the mean epochs 2000.07 and 2001.80, respectively, therefore, we had an opportunity to analyse the spatial correlation between photospheric spots and chromospheric activity. By comparing the variation of chromospheric emission with the light curves in fig. 7 of Lanza et al. (2006), we find a clear anti-correlation: the EWs approach a maximum when V711 Tau becomes fainter and most spots appear on its visible hemisphere. Thus, this indicates that the chromospheric activity region is associated with the photospheric star-spot region in the spatial structure, and further that the localized magnetic loop heating the chromospheric activity region is connected to the spot region.

From Fig. 5, showing chromospheric activity emission in the Hα line against the year of observation, it can evidently be seen that chromospheric activity gradually increases from a deep minimum near 2002, which indicates a long-term variation of chromospheric activity due to the evolution of active structures. In addition, we find that the year of minimum chromospheric activity is very close to the local brightness maximum of V711 Tau, and the behaviour is anti-correlated with the mean brightness variation reported by Berdyugina & Henry (2007) and correlated with the variation in light loss caused by spot activity derived by Muneer et al. (2010). This suggests that the long-term variation of chromospheric activity is also spatially connected with the long-term evolution of photospheric spot regions. The cyclic behaviour for several years of spot activity of V711 Tau was extensively derived by Henry et al. (1995), Lanza et al. (2006), Berdyugina & Henry (2007) and Muneer et al. (2010). Also, a possible chromospheric activity cycle with a period of about 18 yr was found by Buccino & Mauas (2009) based on *International Ultraviolet Explorer* ultraviolet high- and low-resolution spectra from 1975 to 1996, in good agreement with the ones derived from the optical photometric observations mentioned above.

To infer the possible cycle of the flip-flop phenomenon and the longer chromospheric activity variation for V711 Tau, we may require more frequent observations over several years. Fortunately, our project is ongoing.

4.5 Comparison between LQ Hya and V711 Tau

The rapidly rotating single K2 V star LQ Hya and RS CVn-type system V711 Tau are both important target stars in our project. Although rotational rate spins down with age during the evolution of single stars, the evolved K1 IV star of V711 Tau rotates fast due to tidal locking. Based on the similar activity patterns of LQ Hya and RS CVn stars, Berdyugina et al. (2002) concluded that binarity does not have a strong effect on the dynamo and it is the rapid rotation that determines the dynamo behaviour of stars. Our previous results for LQ Hya have similarities to V711 Tau, such as the rotational modulation of chromospheric activity and an association between photospheric spots and chromospheric activity regions (Cao & Gu 2014). Similar results have also been found for four young solar-type stars by Biazzo & Frasca (2007). Although no optical flares were found during our observations, a strong flare on LQ Hya was detected by Montes et al. (1999). Moreover, it can be seen that V711 Tau has much stronger activity than LQ Hya according to the emission levels of chromospheric activity indicators during our observations.

5 CONCLUSIONS

Based on the above analysis of our long-term high-resolution spectroscopic observations taken during eight observing runs from 1998 to 2004, we have obtained information about chromospheric activity of the very active RS CVn-type system V711 Tau with several optical activity indicators formed at different atmospheric heights. Our main results are summarized as follows:

(i) Strong and variable chromospheric emission in the Hα and Ca II IRT lines indicates that V711 Tau is a very active system. Most of the chromospheric emission is attributed to the primary star of the system. The secondary component also has weak emission, but it is less active. The ratio of excess emission EW$_{8542}$/EW$_{8498}$ indicates that Ca II IRT emission arises predominantly from plage-like regions, like several other RS CVn-type stars.

(ii) Two optical flare-like events were detected in the 2000 September and 2004 November observing runs, which were confirmed by the He I D$_3$ line emission.

(iii) We have found rotational modulation of chromospheric activity in the Hα and Ca II IRT lines, which suggests the presence of chromospheric activity longitudes over the surface of V711 Tau. Two active longitudes separated by about 180° were observed to dominate the activity during our observations excluding 2004 February, and one flip-flop event occurred.

(iv) The chromospheric activity level shows a long-term variation, which gradually increases from a deep minimum near the year 2002. This indicates that the evolution of chromospheric activity regions is on a long timescale.

(v) By comparing with the light curves of Lanza et al. (2006) and long-term photometric variations found by Berdyugina & Henry (2007) and Muneer et al. (2010), a close spatial connection between photospheric spots and chromospheric active regions for short and long timescales was found for V711 Tau, which indicates the spatial structure of active regions at different atmospheric layers.

Downloaded from http://mnras.oxfordjournals.org/ at National Astronomical Observatory on November 29, 2015

ACKNOWLEDGEMENTS

We are grateful to Dr Montes for providing a copy of the STARMOD program. We thank Prof Xiaojun Jiang and Prof Jianyan Wei for allocating observing time to our project, and the staff of the 2.16-m telescope of Xinglong station of the National Astronomical Observatories for their help and support during our observations. We would like to thank the anonymous referee for helpful comments and suggestions, which significantly improved our manuscript. This work is supported by National Natural Science Foundation of China under grants 10373023, 10773027 and 11333006, and the Chinese Academy of Sciences through project KJCX2-YW-T24.

REFERENCES

Barden S. C., 1985, ApJ, 295, 162
Berdyugina S. V., Henry G. W., 2007, ApJ, 659, L157
Berdyugina S. V., Berdyugin A. V., Ilyin I., Tuominen I., 1998, A&A, 340, 437
Berdyugina S. V., Ilyin I., Tuominen I., 1999, A&A, 349, 863
Berdyugina S. V., Pelt J., Tuominen I., 2002, A&A, 394, 505
Biazzo K., Frasca A., 2007, ApJ, 656, 474
Buccino A. P., Mauas P. J. D., 2009, A&A, 495, 287
Cao D.-T., Gu S.-H., 2012, A&A, 538, 130
Cao D.-T., Gu S.-H., 2014, AJ, 147, 38
Catalano S., Rodonò M., Frasca A., Cutispoto G., 1996, in Strassmeier K. G, Linsky J. L., eds, Proc. IAU Symp. 176, Stellar Surface Structure. Kluwer, Dordrecht, p. 403
Chester M. M., 1991, PhD thesis, Pennsylvania State Univ.
Dempsey R. C., Neff J. E., Thorpe M. J., Linsky J. L., Brown A., Cutispoto G., Rodonò M., 1996, ApJ, 470, 1172
Donati J.-F., 1999, MNRAS, 302, 457
Donati J.-F., Brown S. F., Semel M., Rees D. E., Dempsey R. C., Matthews J. M., Henry G. W., Hall D. S., 1992, A&A, 265, 682
Donati J.-F. et al., 2003, MNRAS, 345, 1145
Ducati J. R., 2002, VizieR Online Data Catalog, 2237, 0
Eggen O. J., 1978, Inf. Bull. Var. Stars, 1426, 31
Fekel F. C., 1983, ApJ, 268, 274
Foing B. H. et al., 1994, A&A, 292, 543
Frasca A., Biazzo K., Taş G., Evren S., Lanzafame A. C., 2008a, A&A, 479, 557
Frasca A., Kovari Zs., Strassmeier K. G., Biazzo K., 2008b, A&A, 481, 229
Gálvez M. C., Montes D., Fernández-Figueroa M. J., De Castro E., Cornide M., 2009, AJ, 137, 3965
García-Alvarez D. et al., 2003a, A&A, 397, 285
García-Alvarez D., Barnes J. R., Collier Cameron A., Doyle J. G., Messina S., Lanza A. F., Rodonò M., 2003b, A&A, 402, 1073
Gondoin P., 1986, A&A, 160, 73
Gu S.-H., Tan H.-S., Shan H.-G., Zhang F.-H., 2002, A&A, 388, 889
Gu S.-H., Collier Cameron A., Barnes J. R., Yang J.-Y., 2007, in Hartkopf W. I., Guinan E. F., Harmanec P., eds, Proc. IAU Symp. 240, Binary Stars as Critical Tools and Tests in Contemporary Astrophysics. Cambridge Univ. Press, Prague, p. 714
Gunn A. G., Doyle J. G., 1997, A&A, 318, 60
Gunn A. G., Doyle J. G., Houdebine E. R., 1997, A&A, 319, 211
Hall J. C., 1996, PASP, 108, 313
Henry G. W., Eaton J. A., Hamer J., Hall D. S., 1995, ApJS, 97, 513
Lanza A. F., Piluso N., Rodonò M., Messina S., Cutispoto G., 2006, A&A, 455, 595
López-santiago J., Montes D., Fernández-Figueroa M. J., Ramsey L. W., 2003, A&A, 411, 489
Montes D., Fernández-Figueroa M. J., De Castro E., Cornide M., 1995a, A&A, 294, 165
Montes D., Fernández-Figueroa M. J., De Castro E., Cornide M., 1995b, A&AS, 109, 135
Montes D., Fernández-Figueroa M. J., De Castro E., Sanz-Forcada J., 1997, A&AS, 125, 263
Montes D., Saar S. H., Collier Cameron A., Unruh Y. C., 1999, MNRAS, 305, 45
Montes D., Fernández-Figueroa M. J., De Castro E., Cornide M., Latorre A., Sanz-Forcada J., 2000, A&AS, 146, 103
Muneer S., Jayakumar K., Rosario M. J., Raveendran A. V., Mekkaden M. V., 2010, A&A, 521, A36
Petit P. et al., 2004, MNRAS, 348, 1175
Schrijver C. J., Zwaan C., 2000, Solar and Stellar Magnetic Activity. Cambridge Univ. Press, Cambridge
Strassmeier K. G., Bartus J., 2000, A&A, 354, 537
Vogt S. S., Penrod G. D., 1983, PASP, 95, 565
Vogt S. S., Hatzes A. P., Misch A. A., Kürster M., 1999, ApJS, 121, 547
Wood B. E., Harper G. M., Linsky J. L., Dempsey R. C., 1996, ApJ, 458, 761
Zhai D. S., Zhang X. B., 1996, A&A, 309, 530
Zhang L.-Y., Gu S.-H., 2008, A&A, 487, 709
Zhao G., Li H.-B., 2001, Chinese J. Astron. Astrophys., 1, 555
Zirin H., 1988, Astrophysics of the Sun. Cambridge Univ. Press, Cambridge

This paper has been typeset from a TEX/LATEX file prepared by the author.

Downloaded from http://mnras.oxfordjournals.org/ at National Astronomical Observatory on November 29, 2015